A comparison between wet HF etching and vapor HF etching for sacrificial oxide removal

A. Witvrouw[a], B. Du Bois[a,b], P. De Moor[a], A. Verbist[a], C. Van Hoof[a], H. Bender[a] , Kris Baert[a]

[a] IMEC, Kapeldreef 75, B-3001 Leuven, Belgium

[b] Departement Rega, Katholieke Hogeschool Leuven, St. Maartensstraat 55d, B - 3000 Leuven, Belgium

ABSTRACT

In this work the etching of different Si-oxide (thermal oxide, TEOS as –deposited, TEOS annealed and PSG annealed), Si-nitride (LPCVD and PECVD) and metal layers (Al-Cu, Ti and TiN) in HF:H_2O 24.5:75.5, BHF:glycerol 2:1 and vapor HF is studied and compared. The vapor HF etching is done in a commercially available system for wafer cleaning, that was adapted according to custom specifications to enable stiction-free surface micro-machining. The etch rates as a function of etching method, time and temperature (for HF vapor) are determined. Moreover, the influence of internal (temperature, nitrogen flow, wafer size) and external (sample pretreatment) parameters on the HF vapor etching process are analyzed before choosing the standard HF vapor etch technique used for comparing the etching behavior of the different films.

Auger depth profiles and infrared spectroscopy are used to explain the time varying etch rates of the metal films and the changes in the Si-nitride films after HF vapor etching.

Keywords: surface micro-machining, HF vapor, sacrificial etching

1.INTRODUCTION

Surface micro-machined Micro Electro Mechanical Systems (MEMS) are often made by using poly-Si or poly-SiGe [1,2] as a structural layer and an oxide layer as the sacrificial layer. The sacrificial layer can then be etched with high selectivity towards the structural layer by the use of Hydrogen Fluoride (HF). The most widespread method of HF based etching is wet chemical etching in a mixture of HF and water or in a mixture of buffer HF with glycerol [3-10]. The latter is preferred when Aluminum structures are on the wafer as the addition of glycerol to BHF decreases the etch rate of metals. Drying of released wet etched structures however causes problems of stiction. Although solutions exist to overcome these problems, it is also possible to circumvent stiction by using an HF vapor release etch. Especially when the wafer temperature during the release is raised above 40 °C, a high yield can be obtained for the surface micro-machined structures [11]. An example of a surface micromachined poly-SiGe bolometer, fabricated by sacrificial etching of TEOS with HF vapor, is shown in figure 1.

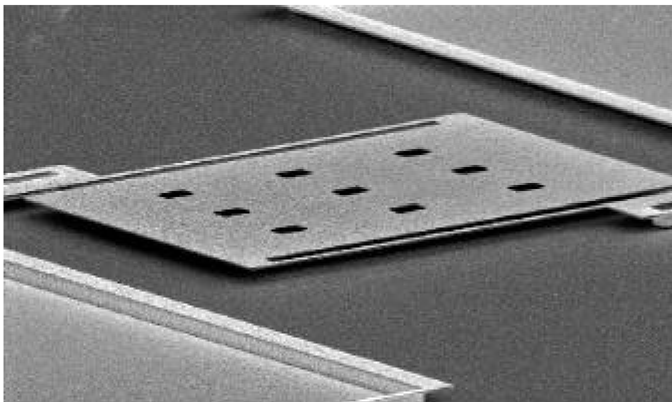

Figure 1: surface micromachined poly-SiGe bolometer pixel [1].

2. EXPERIMENTAL PROCEDURE

2.1. Sample preparation

The blanket layers that were investigated in this work are four different Si-oxides, two different Si-nitrides and three metal-based films. The Si-oxide layers are 1200 nm wet thermal oxide grown at 975 °C, 1000 nm TEOS (tetraethoxysilaan) deposited by a CVD process at 670 °C, the same film annealed for 30 min. at 900 °C and 1000 nm PSG (phosphosilicate glass) with 4.5 wt.% P grown at 550 °C and annealed for 30 min at 750 °C. The 200 nm thick LPCVD nitride layer was deposited at 770 °C, while the 1000 nm PECVD nitride was deposited at 400 °C. The metal-based films are all deposited by sputter deposition. The titanium and titaniumnitride films are 200 nm thick and the Al - 0.5 wt.% Cu film is 1000 nm thick. All these layers are commonly used in semiconductor and MEMS processing and can thus be present on the wafer during the sacrificial oxide etching.

2.2. Description etch procedure

For the wet chemical etching experiments two different solutions were used. The first solution consists of one part HF (49 %) and one part DI water, resulting in a 24.5% HF solution in water or 14.2 mol/l. The second solution is made by mixing two parts of buffer HF (BHF) with one part glycerol ($HOCH_2$-HOCH-CH_2OH). BHF itself consists of seven parts of NH_4F (40%) and one part HF (49%). The BHF/glycerol solution thus has lower concentration of HF, only 4 % or 9.4 mol/l. The etching will thus go slower for the BHF/glycerol mixture compared to the HF/H_2O mixture, but will also be more selective as will become clear from the measurements. The experimental procedure used for the wet etching is as follows: after etching a piece of a 200 mm wafer for a certain time in one of the solutions, the sample is put in a beaker with DI water for a few seconds after which it is rinsed in streaming DI water. After drying with a nitrogen gun, the film thickness is then measured on at least five different places on the wafer. For the transparant films this is done by a spectrometer, for the conductive films this is done indirectly through a sheet resistance measurement. If the film resistivity is assumed to be constant, the sheet resistance is inversely proportional to the film thickness.

The vapor HF etching is done in a commercially available system (Figure 2) for wafer cleaning, that was adapted according to custom specifications to enable stiction-free surface micro-machining. This custom adaptation consisted of adding a heater stage (room temperature to 75 °C) for the wafer. Heating the wafer does result in a slower etching rate (see further), but also allows for stiction free processing [11] as most of the water in the system is evaporated. To get a vapor of HF and water in the reaction hood, which is at a slightly lower pressure than the atmosphere, nitrogen is bubbled through a 49% HF solution. The nitrogen flow can be adjusted between 0.1 and 1 l/min. In order to get reproducible etching results, the preparation of the sample is important (see also 4.1). The samples are first cleaned in water, then dryed with a nitrogen gun and then baked out in a furnace at 120 °C for 30 minutes. This results in a clean sample, which is then preheated for 10 minutes in the system before the etching with a nitrogen flow of 1 l/min starts. Layer thickness measurements are done in the same way as for the wet etched samples.

The reaction equations both for wet [3-10] and vapor HF [13-17] etching can be found in several references. For HF vapor etching it is important to note that surface adsorbed water is needed as an initiator for the HF vapor etching reaction [11,17]. This explains a number of the HF vapor test results described in chapter 4.

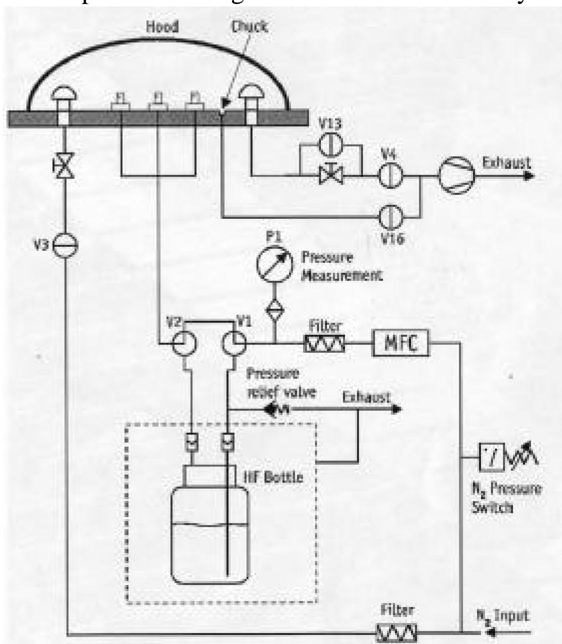

Figure 2: Schematic of the HF-vapor equipment [12].

3.WET CHEMICAL ETCHING

3.1. Si-oxides

3.1.1. Si-oxides in HF/H_20 solution

From all investigated oxides, annealed PSG is etched the fastest in HF/H_2O (Figure 3). The addition of phosphorus, which is converted to phosphoric acid during etching, in PSG increases the etch rate [18,19]. TEOS is etched almost as fast as PSG. Annealing the TEOS densifies the film and makes it more etch resistant. Thermal oxide, the oxide that has seen the highest temperature, is etched the slowest.

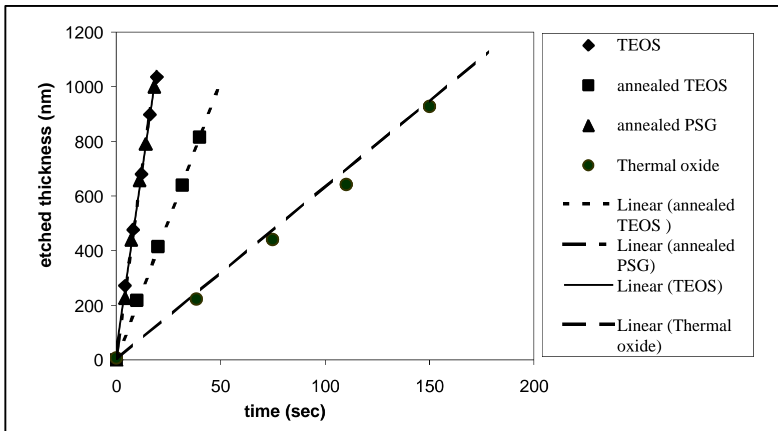

Figure 3: Etch rate of different oxides in HF/H_2O solution

3.1.2. Si-oxides in Buffer HF/glycerol solution

In BHF/glycerol oxides are etched a lot slower compared to in HF/H_2O (Figure 4). As mentioned before, this is due to the lower HF concentration. Moreover, TEOS is etched now slower than annealed PSG. This is probably due to the lower water content in BHF/glycerol, as the reaction of P_2O_5 to phosphoric acid needs water [18].

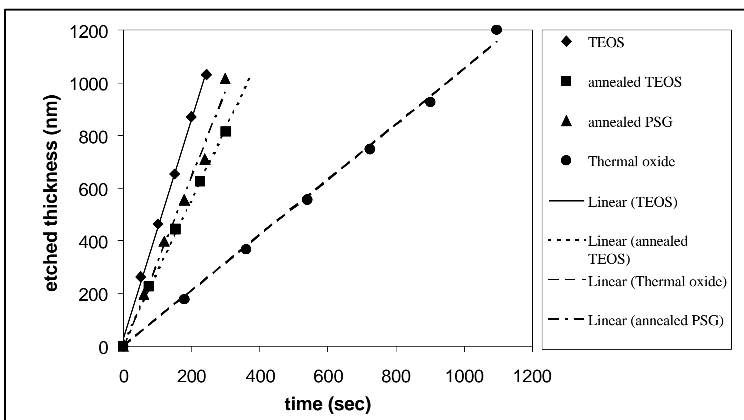

Figure 4: Etch rate of different oxides in BHF/glycerol solution

3.2. Si-nitrides

3.2.1. Si-nitrides in HF/H_20 solution

LPCVD nitride is etched slower than PECVD nitride (Figure 5) due to its higher processing temperature and consequently higher density.

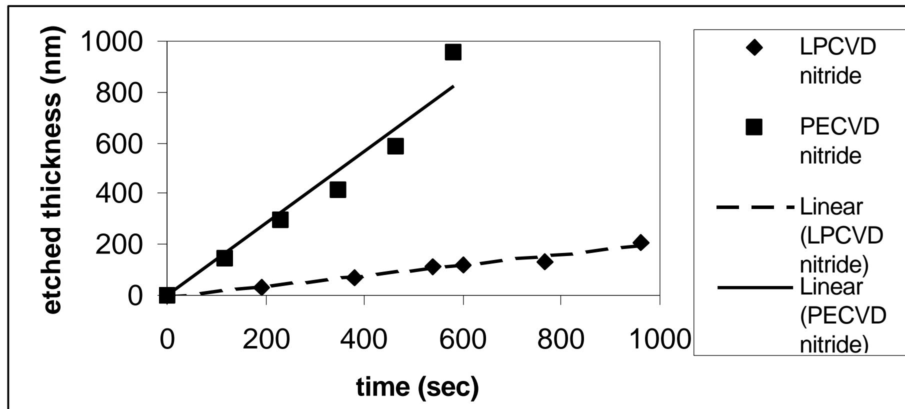

Figure 5: Etch rate of different nitrides in HF/H_2O solution

3.2.2. Si-nitrides in Buffer HF/glycerol solution

Also in BHF/glycerol, PECVD nitride is etched faster than LPCVD nitride (Figure 6). However, the absolute etch rates are reduced substantially compared to etching in HF/H_2O.

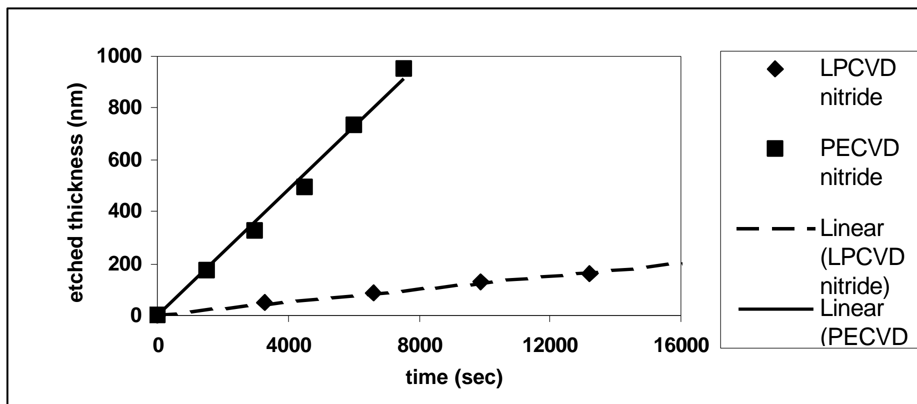

Figure 6: Etch rate of different nitrides in BHF/glycerol solution

3.3. Metals

3.3.1. Metals in HF/H_20 solution

Both Ti and Al-Cu are etched quickly in a HF/H_20 solution (Figure 7a). For TiN, which is made by reactive sputtering of Ti in a nitrogen atmosphere, the etch rate is reduced substantially (Figure 7b). The changes in relative sheet resistance (=R

$_{0,sheet}/R_{sheet} = d/d_0$ for a constant resistivity with R_{sheet} and d, respectively, the sheet resistance and thickness of the film at a certain time, respectively, and $R_{0,sheet}$ and d_0 , respectively, the initial sheet resistance and thickness, respectively) of these metal-based films with etch time is not linear. To get a better understanding of the etching mechanism, Auger depth profiles were taken both for as-deposited and etched films. For Ti it is clear from figures 8a and b that, during the etching, the top Ti layer is converted to a Ti-oxide layer. The same could be seen for the TiN samples. This conversion to an oxide layer results in an increase of resistivity and thus also an increase in sheet resistance. Thus, the changes in sheet resistance measured for Ti and TiN are not directly reflecting changes in film thickness, but mere changes in resistivity. The calculated etch rates in table 1 (see further) are thus only indicative of the rate of attack of the Ti and TiN films. Auger depth profiles for Al-Cu, on the other hand, indicated that the changes in sheet resistance agree very well with the changes in Al-Cu thickness. The only compositional change was a Cu enrichment at the film surface after etching. This indicates that Cu is etched a lot slower than Al. As the Cu remained on the surface, no increase in resistivity is expected and the changes in sheet resistance are therefore a good measure for the changes in film thickness.

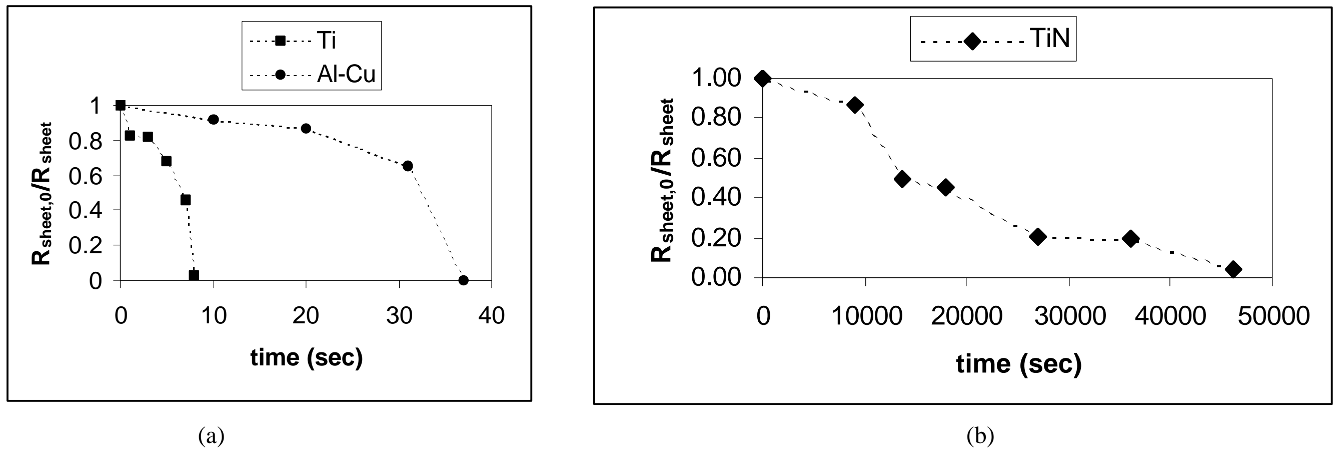

(a) (b)

Figure 7: Relative sheet resistance changes as a function of etching time for Ti and Al-Cu (a) and TiN (b) in an HF/H_2O solution.

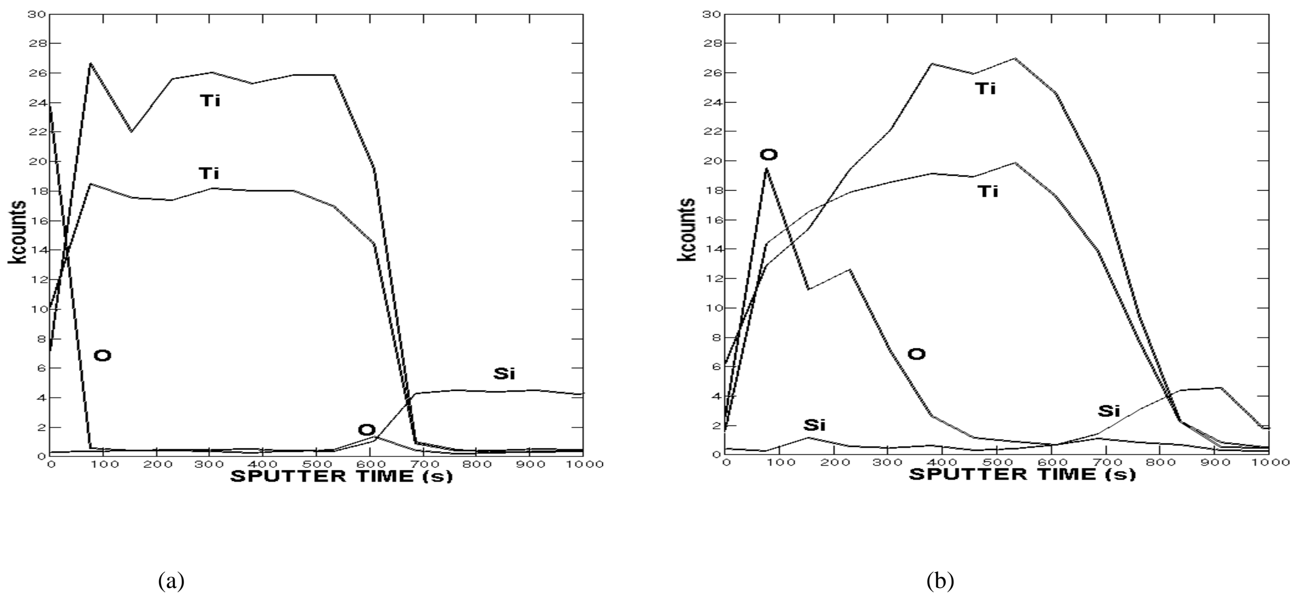

(a) (b)

Figure 8: Auger depth profile of Ti (a) before and (b) after etching for 7 sec in HF/H_2O

3.3.2. Metals in Buffer HF/glycerol solution

The investigated metal-based films are etched a lot slower in the BHF/glycerol solution (Figure 9 a and b). This is exactly the reason why this solution is preferred for sacrificial oxide etching when metal films are on the sample surface. Only Ti is still etched relatively fast.

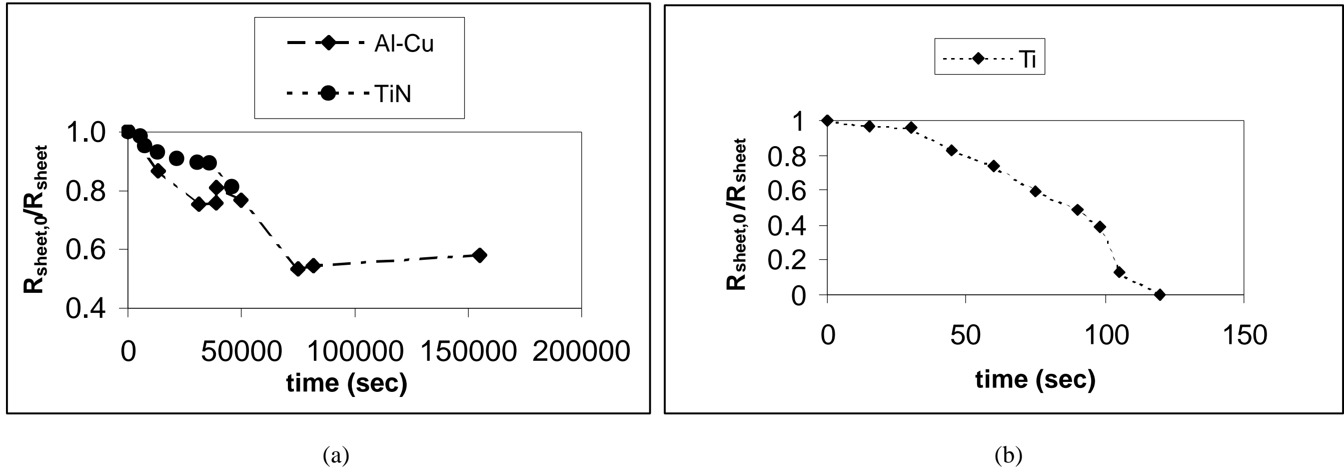

(a) (b)

Figure 9: Relative sheet resistance changes as a function of etching time for TiN and Al-Cu (a) and Ti (b) in a BHF/glycerol solution.

3.4. Conclusion wet etching

The etch rates of the different materials in the two solutions are listed in Table 1. These etch rates were obtained from a linear least squares fit of all data points, with the exception of the metal-based films with the non-linear characteristics. The etch rates of Al-Cu, Ti and TiN were determined from the average changes in sheet resistance with etching time over the whole etching period in the assumption of a constant resistivity. They can thus only be taken as an estimate.

The main conclusions from Table 1 are:

- All etch rates are substantially lower in BHF/glycerol compared to HF/H_2O.
- The BHF/glycerol solution has a much higher selectivity towards nitrides and metal-based films and is therefore more suited as etching solution when the latter materials are on the wafer during the sacrificial oxide etching.
- The difference in etch rate between different types of oxide is larger in the HF/H_2O solution. This solution is thus preferred when oxides need to be etched selectively towards each other.

Material	PSG annealed	TEOS	TEOS annealed	Thermal oxide	PECVD nitride	LPCVD nitride	Al-Cu	Ti	TiN
Etch rate in HF/H_2O [nm/min]	3300± 100	3110 ± 80	1180 ± 10	410 ± 20	98 ± 7	12.8 ± 0.6	800 ± 600	1200 ± 600	0.4 ± 0.2
Etch rate in BHF/ glycerol [nm/min]	198 ± 7	247 ± 4	159 ± 2	66 ± 1	7.6 ± 0.3	0,72 ± 0,02	0.4 ± 0.1 *	60 ± 30	0.06 ± 0.05

Table 1: Etch rate in HF/H_2O and BHF/glycerol solutions.
*This value was determined from the etching data of the first 23 hours only.

4.VAPOR HF

4.1. Influence of internal and external parameters on the HF vapor etching process

Initial tests on HF vapor etching indicated that several parameters, such as the sample pre-heat time and the sample size, had an influence on the HF vapor etch rate. Therefore a series of pre-tests were performed in order to set up a reproducible testing method. The sample preparation itself is crucial as residual water on the sample might accelerate etching [17]. A reproducible way to prepare the samples was described in chapter 2 and has been used for all tests listed below.

4.1.1. Effect of pre-heat time

In Figure 10 the influence of the waiting time between putting the sample on the heater stage and the inlet of the etching vapor is shown. Clearly it takes some time before the sample is at the processing temperature. If one does not wait long enough, the temperature is too low and the etching goes faster (see also 4.1.4). From these results it was decided to set the pre-heat time to 10 min.

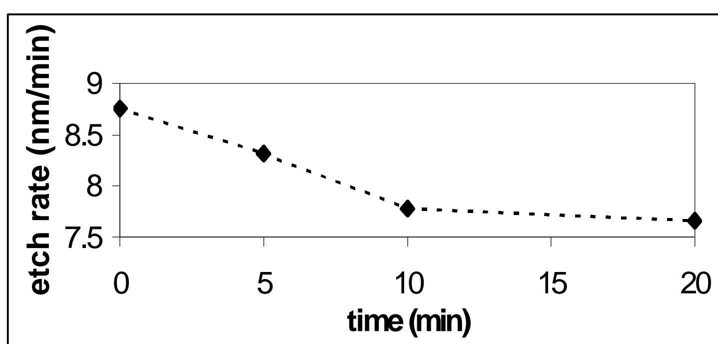

Figure 10: Influence of pre-heat time on the etch rate for 2cmx2cm annealed TEOS samples at a heater stage temperature of 50 °C, a nitrogen flow of 1 l/min and an etching time of 20 min.

4.1.2. Effect of N2-flow

In Figure 11 the increase in etch rate with increasing nitrogen flow is shown. At low flow rates, the supply of reagentia is too low and the etch rate is very low. There is probably not enough water to catalyze the reaction [17]. At medium flow rates an increase in etch rate can be seen with increasing flow. This increase however stops for very large flow rates as at that time the supply of reagentia is probably not etch rate limiting any more.

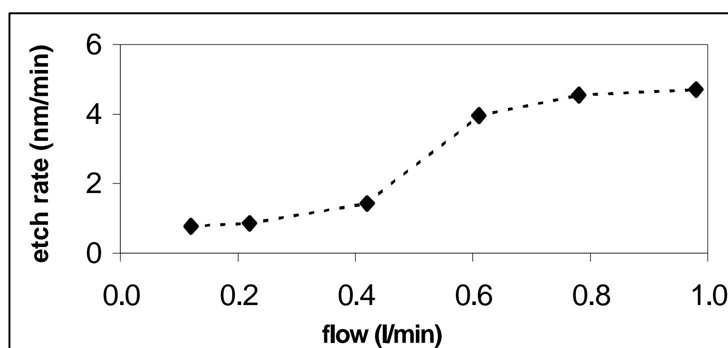

Figure 11: Influence of the nitrogen flow on the etch rate for 2cmx2cm annealed TEOS samples at a heater stage temperature of 50 °C, a pre-heat time of 10 min. and an etching time of 20 min.

4.1.3. Effect of wafer size

In Figure 12, the effect of wafer size on the etch rate is shown. Clearly larger wafer sizes etch slower. This is probably due to the limited supply of reagentia. If it were possible to increase the nitrogen flow more, it might be that this difference in etch rate for different wafer sizes would disappear.

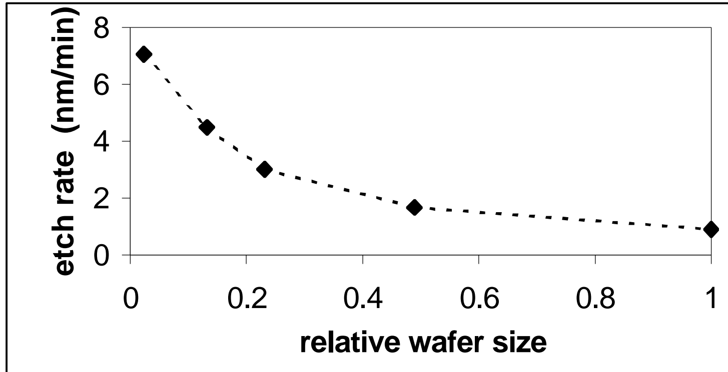

Figure 12: Influence of the wafer size, relative to a 150 mm wafer, on the etch rate for annealed TEOS samples at a heater stage temperature of 50 °C, a nitrogen flow of 1 l/min, a pre-heat time of 10 min and an etching time of 20 min.

4.1.4. Effect of temperature

As expected from literature [11], the etch rate decreases with increasing temperature as the amount of condensed water decreases with increasing temperature. This is a disadvantage of working at elevated temperatures, but on the other hand also the chances for stiction decrease with a decreasing amount of condensed water. Figure 13 shows another interesting phenomenon: the etch rate at 42 °C is lower for a total etch time of 3 min compared to an etch time of 15 min. This can be explained by the fact that the HF vapor etch has an incubation period before etching really starts. The latter was shown in a separate experiment.

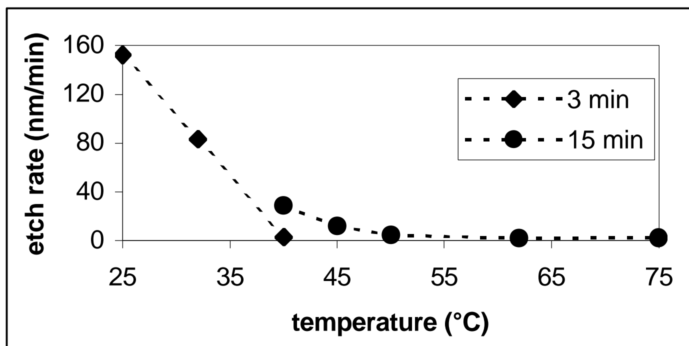

Figure 13: Influence of the temperature on the etch rate for 2cmx2cm annealed TEOS samples at a nitrogen flow of 1 l/min, a pre-heat time of 10 min and an etching time of 3 or 15 min.

4.1.5. Changes in HF concentration

When N_2 bubbles through the HF/H_2O solution, more HF is evaporated than water for a 49% HF solution [17]. This results in a decrease of HF concentration in the solution and thus in a decrease in the etch rate with etching time. For an annealed TEOS sample, for example, the etch rate is decreased by one third after 90 hours of total etching time. This decrease in etch rate has to be taken into account when comparing the etching results of different materials. This was always done for the experiments described in 4.2-4.4.

4.1.6. Test method

To avoid equipment and sample surface dependent etch rate results, always 2cmx2cm samples, a pre-heat time of 10 min, a nitrogen flow of 1 l/min and a heater temperature of 35 °C were used for the experiments of 4.2 - 4.4.

4.2. Si-oxides

Figure 14 shows the etched thickness as a function of etch time in HF vapor for various oxides. Similar to the etching in HF/H_2O, thermal oxide is etched the slowest and annealed PSG the fastest. The etching of annealed PSG also results in a wet residue on the surface (Figure 15). This is probably phosphoric acid, as this only evaporates at 200 °C. Using PSG as a sacrificial layer is thus not a good idea when HF vapor is used for sacrificial etching, as stiction will be unavoidable.

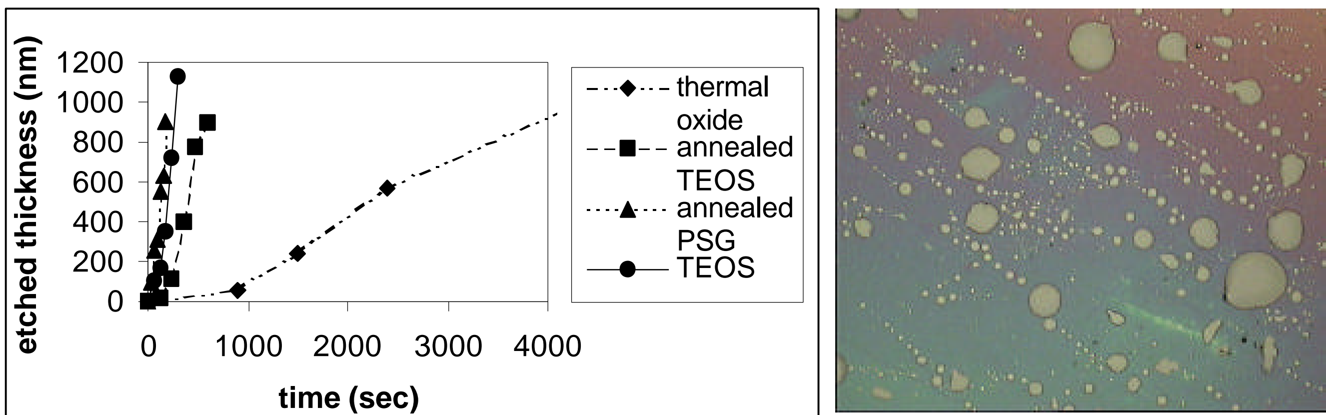

Figure 14: Etch rate of oxides in HF vapor at 35 ºC. The values in the figure are corrected for changes in the HF concentration.

Figure 15: surface of annealed PSG etched for 2 min with HF vapor.

4.3. Si-nitrides

After etching Si-nitride with HF vapor, the thickness could not be measured anymore by ellipsometry. Clearly another compound had formed. Infrared absorption measurements indicated a gradual disappearance of Si-N peaks and a gradual appearance of peaks belonging to $Si\text{-}NH_2$, which might arise from $(NH_4)_2SiF_6$ or from NH_4HF_2, in agreement with the literature [20]. If needed, $(NH_4)_2SiF_6$ can be removed by heating up the wafer after HF-etching [20].

4.4. Metals

All investigated metal-based films are etched very slow in vapor HF (Figure 16). Especially Al-Cu is hardly attacked.

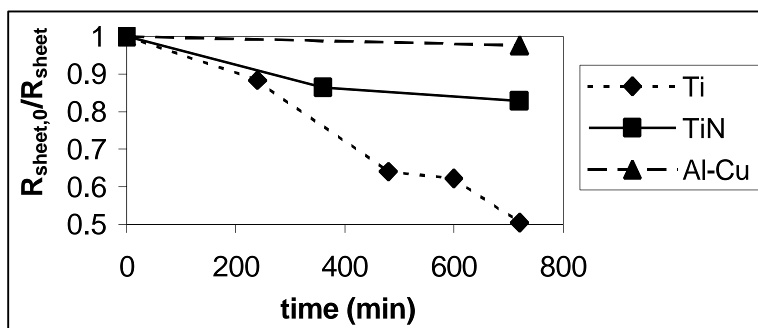

Figure 16: Relative sheet resistance changes as a function of etching time for Ti, TiN and Al-Cu in HF vapor at 35 ºC. The indicated values are as measured, thus without correction for the changes in HF concentration.

4.5. *Conclusion HF vapor etching*

The etch rates of the Si-oxides and metal-based films in HF vapor @ 35 °C are listed in Table 2. The high selectivity towards metal-based films is clear. Moreover, the possibility of stiction-free etching, with the exception of the etching of PSG, makes HF vapor a very attractive sacrificial etching technique. The reaction of the nitrides, however, can be regarded as a disadvantage. Also, the oxide etch rates are, with the exception of PSG, lower than in the BHF/glycerol solution and for all oxides certainly lower than in the HF/H_2O solution.

Material	Annealed PSG	TEOS	Annealed TEOS	Thermal oxide	Ti	TiN	Al-Cu
Etch rate @35°C (nm/min)	290 ± 20	220 ± 40	100 ± 10	15 ± 1	0.19 ± 0.02	0.06 ± 0.02	0.03

Table 2: Etch rates in HF-vapor @ 35°C determined from a linear least square fit through all available data points for one material. The values in the table are corrected for changes in the HF concentration (multiplication factor between 1 and 1.4).

5.DISCUSSION AND CONCLUSION

As a conclusion a table is made (Table 3) of the relative etch rates of the different materials with respect to the thermal oxide etch rate for the three different sacrificial etching techniques. When comparing the selectivities between the different oxides and the selectivity of thermal oxide etching towards Al-Cu and Ti, vapor HF clearly gives the best results. Only when nitrides or PSG are present on the surface, HF vapor might not be such a good choice. Also when fast oxide etching is needed and no selectivity towards other materials is needed, wet etching in an HF/H_2O solution might be preferred. However, in the latter case one needs to solve the stiction problems.

Material	Annealed PSG	TEOS	Annealed TEOS	Thermal oxide	PECVD nitride	LPCVD nitride	Ti	Ti nitride	Al-Cu
Relative etch rate in HF/H_2O	8.0	7.6	2.9	1	0.24	0.03	2.9	0.001	2.0
Relative etch rate in BHF-glycerol	3.0	3.7	2.4	1	0.12	0.01	0.9	0.0009	0.006
Relative etch rate in HF-vapor @ 35°C	19	15	6.7	1			0.01	0.004	0.002

Table 3: Relative etch rates of the different materials with respect to the thermal oxide etch rate in wet HF/H_2O, wet BHF/glycerol and vapor HF @ 35°C.

6.ACKNOWLEDGEMENTS

The authors thank P. Van Marcke for the FTIR measurements and C. Drijbooms for the Auger spectroscopy.

7.REFERENCES

1. P. De Moor, S. Sedky, D. Sabuncuoglu, C. Van Hoof, 'Linear arrays of uncooled poly SiGe microbolometers for IR detection', Proc. SPIE Vol. 3876, p. 256-259, 1999.

2. S. Sedky, P. Fiorini, M. Caymax, S. Loreti, K. Baert, L. Hermans, 'Structural and Mechanical Properties of Polycrystalline Silicon germanium for Micromachining Applications', J. of Microelectromechanical Systems, **7** (4), 1998, pp. 365-372.

3. D.J. Monk, D.S. Soane, R.T. Howe, "Sacrificial layer SiO_2 wet etching for micromachining applications", Transducers, juni 24-27, p. 647-650, 1991.

4. D.J. Monk, D.S. Soane, "Determination of the etching kinetics for the hydrofluoric acid/silicon dioxide system", J. Electrochem. Soc., vol 140, nr. 8, p. 2339-2345, Augustus 1993.

5. J.S. Judge, "A study of the dissolution of $Si0_2$ in Acidic Fluoride Solutions", J. Electrochem. Soc., vol 118, nr. 11, p. 1772-1775, 1971.

6. K.R. Williams, R.S. Muller, "Etch Rates for Micromachining Processing", J. Electrochem. Soc., vol 5, nr. 4, p. 256-269, 1996.

7. R.A. Haken, I.M. Baker, J.D.E. Benyon, "An investigation into the dependence of the chemically-etched edge profiles of silicon dioxide on etchant concentrations and temperature", Thin Solid Films, vol. 18, nr. 1, p. S3-S6, Oktober 1973.

8. W.R Runyan, K.E. Bean , "Semiconductor Integrated Circuit Processing Technology", MA: Addison -Wesley, 1990.

9. H. Kikyuama, K. Saka, J. Takano, I. Kawanabe, M. Miyashita, T. Ohmi, "Principles of wet chemical processing in ULSI microfabrication", IEEE Trans. Semicond. Manufact., vol 4, nr.1, p. 26-35, Februari 1991.

10. T.A. Lober, R.T. Howe, "Surface-miromachining processes for electrostatic microactuator fabrication", IEEE, p.59-62, 1988.

11. M. Offenberg, B. Elsner and F. Laermer, 'Vapor HF etching for sacrificial oxide removal in surface micromachining' Proc. Electrochemical Soc. Fall Meeting, vol. 94, no. 2, Oct. 1994, pp. 1056-1057.

12. Operation Manual Pad Fume of Gemetec, figure 2.3.

13. D.F. Weston and R.J. Mattox, 'HF vapor phase etching (HF/VPE): Production viability for semiconductor manufacturing and reaction model' J. Vac. Sci. Technol. **17** (1), 1980, pp. 466-469.

14. S. Onishi, K. Matsuda and K. Sakiyama, 'A Mechanism of Particle Generation and a Method to Suppress Particles in Vapor HF/H_2O System', Extended Abstracts of the 22nd Conference on Solid State Devices and Materials, 1990, pp. 1127-1130.

15. P.A.M. van der Heide, M.J. Baan Hofman and H.J. Ronde, 'Etching of thin SiO_2 layers using wet HF gas', J. Vac. Sci. Technol. **A 7** (3), 1989, pp. 1719-1723.

16. P.J. Holmes and J.E. Snell, 'A Vapour Etching Technique for the Photolithography of Silicon Dioxide' Microelectronics and reliability **5**, 1966, pp. 337-341.

17. C.R. Helms and B.E. Deal, 'Mechanisms of the HF/H_2O vapor phase etching of SiO_2', J. Vac. Sci. Technol. **A 10** (4), 1992, pp. 807-811.

18. W.I. Jang, C.A. Choi, C.S. Lee, Y.S. Hong and J.H. Lee, 'Characteristics of Residual Products in HF Gas-phase Etching of sacrificial Oxides for Silicon Micromachining, Proc. Symp. on Design, Test and Microfabrication of MEMS and MOEMS, SPIE **3680**, pp. 956-963 (1999).

19. D.J. Monk, D.S. Soane, R.T. Howe, 'Hydrofluoric acid etching of silicon dioxide sacrificial layers. I. Experimental observations', J. Electrochem. Soc., **141** (1), pp. 264-269 (1994).

20. G. Vereecke, M. Schaekers, K. Verstraete, S. Arnauts, M.Heyns and W. Plante, 'Quantitative Analysis of trace metals in Silicon Nitride Films by a Vapor Phase Decomposition/Solution Collection Approach', J. Electrochem. Soc., **147** (4), pp. 1499 – 1501 (2000).